nature communications

Article

https://doi.org/10.1038/s41467-024-51769-w

An economic demand-based framework for prioritization strategies in response to transient amino acid limitations

Received: 1 September 2023

Accepted: 15 August 2024

Published online: 23 August 2024

Check for updates

Ritu Gupta[1,3,4], Swagata Adhikary[1,2,4], Nidhi Dalpatraj[1] & Sunil Laxman[1]

Cells contain disparate amounts of distinct amino acids, each of which has different metabolic and chemical origins, but the supply cost vs demand requirements of each is unclear. Here, using yeast we quantify the restoration-responses after disrupting amino acid supply, and uncover a hierarchically prioritized restoration strategy for distinct amino acids. We comprehensively calculate individual amino acid biosynthetic supply costs, quantify total demand for an amino acid, and estimate cumulative supply/demand requirements for each amino acid. Through this, we discover that the restoration priority is driven by the gross demand for an amino acid, which is itself coupled to low supply costs for that amino acid. Demand from metabolic requirements dominate the demand-pulls for an amino acid, as exemplified by the largest restoration response upon disrupting arginine supply. Collectively, this demand-driven framework that drives the amino acid economy can identify novel amino acid responses, and help design metabolic engineering applications.

Cells respond to changes in nutrients, by rewiring global processes towards restoring homeostasis. Cell metabolism has therefore been viewed as an economy, with the ability to manage metabolite supply in proportion to their requirements towards different allocations[1–3]. In any economy, such a 'metabolic factory' would not merely synthesize different metabolites to satisfy its activities, but also ensure that each of these is supplied in the right quantities at the right time[4]. Cells therefore must match this required supply with demand through coordinated responses. Indeed, several global metabolic programs regulate cell growth in the context of different nutrient environments[5–9]. While such programs are well known, we have a minimal understanding of how cells prioritize the restoration of distinct metabolic resources when there are transient disruptions in their supply.

Amino acids are the core of a cellular economy, by being essential for protein synthesis as well as metabolism. The relative scale of the latter is particularly underappreciated. Therefore, all cells have multiple mechanisms to sense amino acid sufficiency and/or restore amino acids. A cell incapable of considering supply parameters as well as the demand for a molecule would struggle to survive[1,2]. For example, in eukaryotic cells, the activity of the target of rapamycin complex 1 (TORC1) is high during amino acid sufficiency, and functions as a demand sensor[10,11]. Contrastingly, the Gcn4/ATF4 transcription factor (a master regulator of amino acid biosynthesis) functions during starvation or growth, to restore amino acid supply to match demand[12–14]. When the supply of amino acids is disrupted (causing supply-demand mismatches), we do not understand the prioritization strategies to restore distinct amino acid pools. Commonly, studies utilize complete amino acid starvation, which will treat all amino acids uniformly[6,9,15]. However, amino acids each have distinct metabolic origins and synthesis routes[16,17], chemical properties, uses, and intracellular concentrations[18], and cells might therefore differently prioritize restoring the supply for distinct amino acids after disruptions in supply.

[1]Institute for Stem Cell Science and Regenerative Medicine (inStem), GKVK Post Bellary Road, Bangalore, India. [2]Manipal Academy of Higher Education, Manipal, India. [3]Present address: Section on Nutrient Control of Gene Expression, Division of Molecular and Cellular Biology, Eunice Kennedy Shriver National Institute of Child Health and Human Development, NIH, Bethesda, MD, USA. [4]These authors contributed equally: Ritu Gupta, Swagata Adhikary.
e-mail: sunil@instem.res.in

In this study, using prototrophic yeast cells in a defined glucose and nitrogen replete environment, and by disrupting exogenous amino acid supply, we asked how cells prioritize restorations for distinct amino acids. We organized amino acids into groups based on both their metabolic origins and chemical properties, transiently disrupted the supply of each group, and used reporters to assess amino acid supply-demand mismatches. Through this, we uncover hierarchically prioritized restoration responses to disruptions in the supply of distinct amino acid groups. We estimated the unit costs of biosynthesis to supply each amino acid, separately calculated the relative demand for each amino acid (coming from allocations towards metabolism as well as the proteome), and contextually assessed priorities of amino acid restorations. Our results reveal an amino acid economy where restorations are prioritized based on demand-driven pulls. These findings suggest that demand-dependent economic constraints shape amino acid allocations in cells and suggest the need for distinct amino acid sensing/restoring machinery. This knowledge could be leveraged for efficient metabolic engineering of cells.

Results

A metabolic origin and chemical structure based grouping of amino acids

Cells receive their supply of amino acids from various extrinsic sources, as well as via de novo synthesis from carbon and nitrogen precursors. The demands for amino acids come primarily from protein synthesis, as well as their various uses in metabolism[19,20], as illustrated in Fig. 1A. Transient disruptions in amino acid supply can be achieved by restricting extrinsic sources. If this occurs, we wondered if cells might prioritize the restoration of distinct amino acids (based on demand or supply criteria), or whether they would treat the disruption of all amino acids uniformly (Fig. 1A). Currently, this has not been systematically assessed.

In order to investigate such putative prioritization responses, we had to first pool amino acids into reasonable groups. Conventional amino acid groupings are based on physicochemical properties (Fig S1A), and therefore do not include considerations of their (metabolic) supply or origins. We initially hypothesized that having groups that included supply criteria might help to systematically address this question. We therefore organized amino acids into groups that considered their metabolic origins (as obtained from KEGG[17]), as well as retained information on their chemical structures. This reorganization, consistent with existing metabolic groupings[21], also acknowledges conventional chemical structure based criteria. With such a grouping, it was immediately apparent that the ability to supply precursors for a given amino acid is not uniform, and depends on available precursors given the metabolic state of the cell. Through this, we categorize the different amino acids into seven groups, as shown in Fig. 1B. For completeness the predominant metabolic pathway for each amino acid (in a glucose and nitrogen replete environment), where all precursors used in each pathway are listed, are provided in the composite supplementary Fig. S2. Additional points were considered for specific amino acid groupings. Isoleucine is derived from OAA (oxaloacetate), which comes from either/or pyruvate and TCA cycle/glyoxylate shunt, depending on the metabolic state. In a glucose replete environment, this will predominantly be from pyruvate. The biosynthesis of branched-chain amino acids (BCAAs) are interconnected, with shared enzymes. Therefore, the BCAA group is listed as *glycolytic/ TCA, BCAA group*. Ser, Gly and Ala are all derived from the lower arm of glycolysis, and are therefore called *glycolytic, uncharged* (although ser is polar). We separated the PPP-*dependent* amino acids. Phe, Tyr, and Trp are aromatic and share a common precursor–chorismate–via erythrose 4-phosphate- and can be grouped as *PPP, aromatic*. These however are not fully PPP derived, since they do not require the oxidative arm of the PPP, as long as erythrose 4-phosphate is available[22], however in a glucose replete environment this will predominantly come from the PPP (Supplementary Fig S2). The exclusively PPP derived amino acid is histidine, which is polar and basic, and is grouped separately as *PPP, polar, basic*. The other group is derived from TCA cycle, mainly from OAA and α-ketoglutarate. Glu and Gln are directly derived from α-ketoglutarate. The remaining (Asp, Asn, Thr) also require OAA and are grouped under *TCA, polar* group. The last group (Arg, Pro, Lys) has arginine, proline derived from glutamate, while lysine comes from the glutamate precursor α-ketoglutarate and is grouped alongside arginine due to similar chemical properties. Therefore, we group these together as *glutamate derived* (also see Supplementary Fig. S2). Cysteine and methionine group are *sulfur containing*, and originate from a common precursor—homocysteine. Additionally, glutamate (and glutamine) function through a transamination reaction as an amine donor for other amino acids (Fig. 1C). They thus themselves become a metabolic source for other amino acids. We utilize this grouping shown in Fig. 1B henceforth, to represent the biosynthesis network in our experimental system—a glucose and nitrogen-replete environment. At this stage, we made no further assumptions about any significance of such a grouping.

Cells exhibit hierarchical prioritization responses to supply-disruptions of distinct amino acid groups

With this grouping, we wanted to experimentally assess responses to transient supply disruptions of distinct amino acids. For this, we required a reporter of mismatches in amino acid supply vs demand. Prototrophic yeast cells synthesize all amino acids when provided with nitrogen and carbon precursors, when external amino acid supply is broken. In order to restore amino acid supply, eukaryotic cells utilize the Gcn4/ATF4 transcription factor as a supply-hub to match demand[8,13,15] (Fig. 1D). If cells differentially respond to disruptions in the supply of distinct amino acids, we hypothesized that the Gcn4 activity could correspondingly reflect this response. To investigate this, we shifted yeast cells growing in amino acid-replete medium (+AA), to a defined medium with no free amino acids (-AA), but with ammonium sulfate and glucose. This would disrupt the extrinsic supply, requiring cells to restore supply via de novo amino acid biosynthesis. We monitored the kinetics of Gcn4-activation using an established *Gcn4-luciferase* reporter[23,24], as shown in Fig. 1D. Notably, the reporter activity increases within ~15 minutes of shifting cells to -AA, and peaks at 60–90 min, after which it decreases (Fig. 1E). This 60–90 min window of maximal activity (Fig. 1E) established a precise time-frame for subsequent analyzes and is used henceforth. The kinetics of this observed response would also be consistent with that of a supply-demand coupler, which should increase in activity when supply is below demand, and then decrease as supply matches demand.

We next interrogated how this reporter activity changes when the supply of each amino acid group is disrupted. Cells were grown in +AA medium and shifted to a synthetic medium where each amino acid group was dropped-out, and the other amino acids were supplemented (otherwise performed identically to experiments related to Fig. 1E). Cells were collected at 75 minutes post-shift, and reporter activity estimated. The dropout of any amino acid group induced reporter activity to levels higher than amino acid replete medium (+AA) (Fig. 1F), establishing that Gcn4 reports on supply-demand mismatches for all amino acid groups. However, the extent of reporter induction varied substantially for different amino acid groups (Fig. 1F). Notably, the dropouts of sulfur (Met and Cys), glycolytic/TCA, BCAA (Leu, Ile and Val), glutamate-derived amino acids (Arg, Pro and Lys), and PPP, polar, basic (His) all showed robust reporter activity, comparable to complete amino acid drop out medium (-AA) (Fig. 1F). The dropouts of PPP, aromatic amino acids (Tyr, Trp and Phe), TCA, polar amino acids (Asp, Asn, Glu, Gln and Thr), and glycolytic, uncharged amino acids (Ala, Ser and Gly) showed significantly lower reporter activity (Fig. 1F). This suggests possible prioritizations of restoration responses for distinct amino acid groups.

https://doi.org/10.1038/s41467-024-51769-w

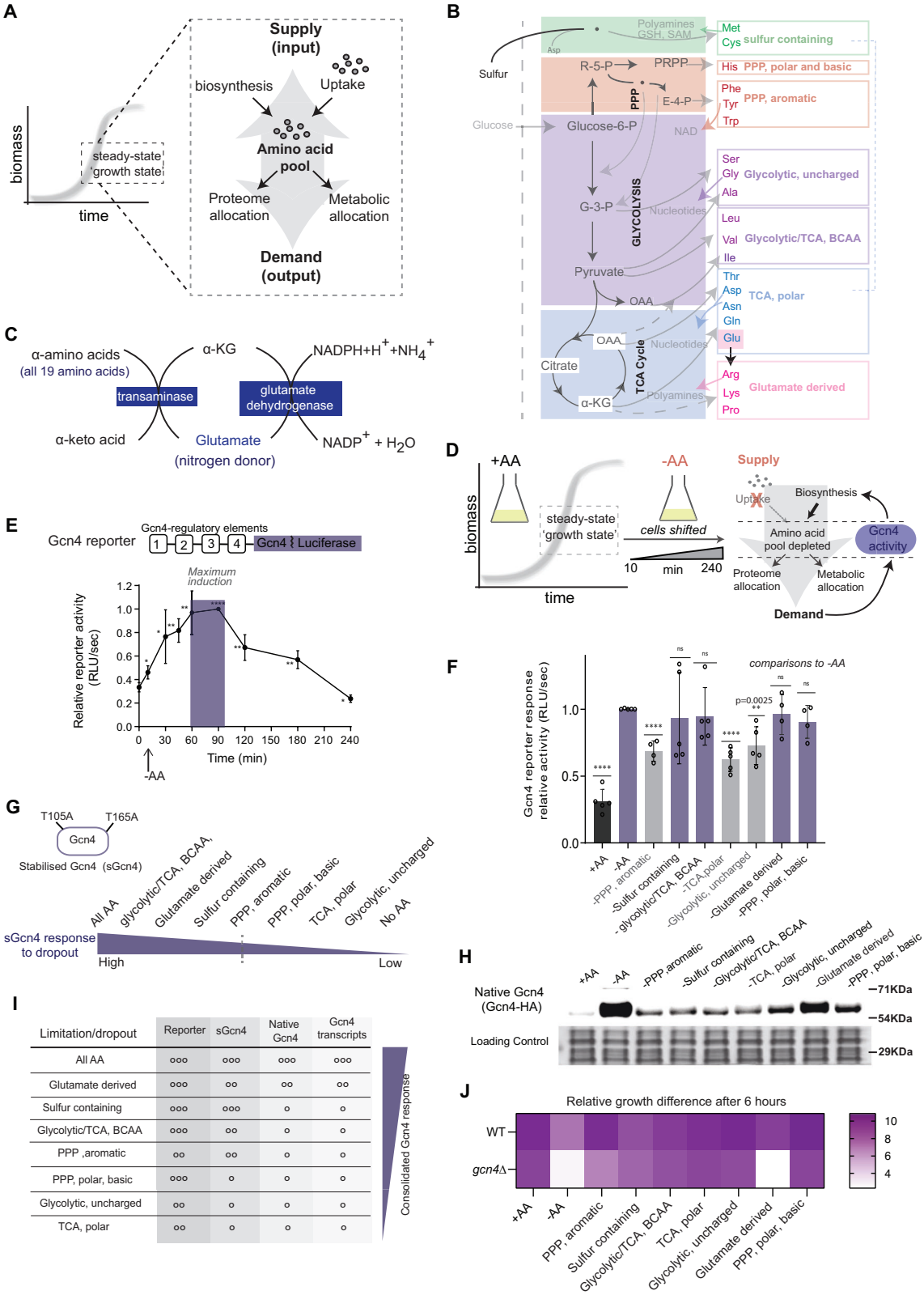

However, as a robust supply-regulator, Gcn4 itself has sophisticated post-transcriptional regulation[13,25,26]. The final Gcn4 output comes from a combination of the translation of upstream regulatory elements of the Gcn4 transcript (as observed with the reporter), and the stability of the Gcn4 protein. For completeness, we further dissected the extent of Gcn4 regulation after limiting the supply of different amino acid groups, by first assessing protein amounts of a stabilized Gcn4 protein (sGcn4-T105A, T165A)[23], and next the native Gcn4 protein. We observed higher sGcn4 protein in dropouts of sulfur containing-, glycolytic/TCA, BCAA - and glutamate-derived amino acids (Supplementary Fig. S1B; lanes 5, 6, 9 and Fig. 1G). The dropout of PPP, aromatic amino acids also showed higher sGcn4 protein levels (Supplementary Fig. S1B; lane 4), and a minimal increase was noted in sGcn4 for the PPP, polar, basic (histidine) dropout (Supplementary Fig.

Fig. 1 | Cells exhibit hierarchical responses to supply-disruptions of amino acid groups notably the glutamate-derived group. A Amino acid supply sources, and demand requirements. Supply comes from de novo biosynthesis and uptake from the environment. Demand includes the use of amino acids for translation and metabolism. **B** A metabolic source and chemical-structure based grouping of amino acids: (i) PPP, aromatic (ii) sulfur containing (iii) Glycolytic/TCA, branched chain amino acids (BCAA) (iv) TCA, polar (v) Glycolytic, uncharged (vi) glutamate derived and (vii) PPP, polar, basic. The locations in the carbon network from which each amino acid is derived are highlighted. See Supplementary Fig. S2 for complete pathways. **C** Single-step transamination of α-ketoglutarate to glutamate (which forms glutamine). Glutamate and glutamine function as a nitrogen source for all amino acids. **D** How amino acid supply-demand mismatches in a batch culture experiment are sensed, managed and restored by Gcn4. **E** Temporal changes in *Gcn4-luciferase* reporter activity, estimating the restoration response to transient amino acid supply disruption. Upper panel: *Gcn4-luciferase* reporter. Data from $n = 3$ (biological replicates) displayed as mean ± SEM. Left to right $p = 0.0324$, 0.0322, 0.0015, 0.0043, <0.0001, 0.0072, 0.0087, 0.0284. **F** Relative *Gcn4-luciferase* reporter activity in the indicated dropout medium (at 75 min), compared to all amino acid dropout (-AA). Data displayed as means ± SEM, $n \geq 4$ biological replicates. For **E** and **F** ****$p < 0.0001$, ns denotes non-significant difference, two-tailed student's t-test. **G** Summary of relative levels of stabilized Gcn4 (sGcn4), in dropout medium (as in panel **F**) at 75 min (also see Supplementary Fig. S1B). **H** Native Gcn4 levels (detected using anti-HA antibody) in the indicated dropout medium, in conditions identical to panels (**F** and **G**). Image represents $n = 3$ biological replicates. **I** Summarized consolidated Gcn4 responses to the supply disruption of each amino acid group. This integrates results from the Gcn4-luciferase reporter, sGcn4, native Gcn4 protein, and Gcn4 dependant transcripts (see Supplementary Fig. S1D). The circles correspond to the intensity of the response. **J** Heat map showing relative cell growth for wild-type and *gcn4*Δ cells in the indicated dropout, after 6 h. Mean for $n = 2$, biological replicates. Data are provided in Source Data file.

S1B; lane 10). These results refined our earlier observations from the reporter, and sGcn4 strongly responds to the disruptions in sulfur containing, glycolytic/TCA, BCAA, glutamate derived, and PPP, aromatic- derived amino acids (Fig. 1G). We also examined native Gcn4 protein after each amino acid group limitations. Native Gcn4 protein was highest after the limitation of the glutamate-derived amino acids (Fig. 1H; lane 8 and Supplementary Fig. S1C). Finally, we estimated direct Gcn4- transcriptional outputs, as an end-point readout for this response. The transcripts of direct Gcn4 targets (obtained from[14]) increased the most in dropout medium for (respectively) sulfur containing-, glycolytic/TCA, BCAA and glutamate-derived amino acids, as well as PPP, aromatic amino acids (Supplementary Fig. S1D, with controls for Gcn4 RNA levels shown in Fig S1E). Through these multiple readouts we construct a consolidated, hierarchically-graded Gcn4 response to supply-disruptions of distinct amino acid groups (Fig. 1I). Cumulatively, the strongest response is to supply-disruptions of glutamate-derived amino acids, followed by strong responses to the drop-out of sulfur containing-, glycolytic/TCA, and BCAA amino acids, a moderate response to PPP, aromatic amino acids, and a minimal response to the glycolytic, uncharged and TCA, polar amino acids in this condition (Fig. 1I).

In complementary experiments, we examined the effect on short-term growth in cells lacking *GCN4* (*gcn4*Δ), when each amino acid group was dropped-out. For this, the growth of wild-type and *gcn4*Δ cells in different amino acid group dropout conditions were monitored. In these cells, the largest relative reduction in growth was observed in the dropout of the glutamate-derived amino acids (Fig. 1J and S1F). Together, these data reveal that upon transient amino acid supply disruption, cells are most constrained by the supply of glutamate-derived amino acids.

Degree of response correlates with low biosynthetic cost and high total demand

We therefore wondered how much the observed responses reflected economic principles of supply and demand. To begin assessing this, we require estimates of individual amino acid supply costs, as well as how much total demand exists for distinct amino acids. Currently, there are no comprehensive costing-scale for amino acids, which accounts for all precursors in a given environment. We therefore devised a scoring-scale to calculate the relative cost to supply an individual molecule of each amino acid. Such a relative scale is more useful and accurate than any absolute scale, and is easy to implement for any nutrient environment. For this scale, we included as many components of cost as possible, accounting for the predominant chemical reactions in each amino acid biosynthetic pathway (in a glucose, ammonium environment). We next computed the *total high-energy phosphate bonds* associated with each amino acid group. For this we included the amino acid precursors, metabolic precursors and reducing equivalents (NAD(P)H) required (as is indicated in Supplementary Fig. S2). Note: the extended metabolic cost calculation details can be found in Appendix 1 (Supplementary information), where every component considered is indicated. The consolidated cost of all amino acid groups therefore collectively comes from the *net* total number of high energy phosphate (ATP) produced (with NADH utilization), concurrent with total NADPH consumed (Supplementary Information Appendix 1, Supplementary Table S4 and Table S5). This is because NADH is utilized in ATP production, while NADPH is concurrently consumed in other steps of amino acid biosynthesis (through reductive biosynthesis)[8]. The results of these comprehensive cost estimations are shown in Fig. 2A, as a relative-cost heat-map scale. Note: in this scoring scale, a lower number indicates a higher cost (Fig. 2A).

From this composite costing scale, we observe that per single molecule cost, the group of glutamate-derived amino acids have the lowest supply costs. From these cost estimations, we also observe that the strongest Gcn4 response (observed for the glutamate-derived group drop-outs) correlates with low amino acid supply costs. To dissect this observation further, we assessed the *individual* costs of each of the glutamate-derived group members - Arg, Lys and Pro, wondering how different they were. Based on individual cost estimations, we found that there were considerable disparities in their individual costs - Arg has the lowest supply costs, Lys has intermediate costs, and Pro has very high costs (Fig. 2B, Appendix I, Supplementary Table S4 and S5). What also becomes clear with this costing-scale is that a composite calculation of supply costs requires scores for all precursors required to make that amino acid. This will change, based on the available nutrient and metabolic state of the cell.

In order to now account for the demand component, we next asked what the composite demand requirement for distinct amino acids were. Currently, there are no relative, order-of-magnitude estimates of demand for amino acids. If we were to break demand down into its components, protein synthesis is one major demand component for amino acids. For estimating the demand coming from only protein synthesis, we analyzed two high-quality ribosome-profiling datasets[27,28] (GEO accession: GSE91068 and GSE122039) from cells grown in comparable, defined-medium conditions. The top 500 most highly translated genes from these datasets were grouped using gene ontology (GO). Expectedly, the most enriched GO category was the ribosomal constituents, consisting of ~25% of the query genes (Supplementary Fig. S3A). This is consistent with our understanding that a majority of proteins in proliferating cells are ribosomal[29]. Next, we calculated the percentages of lysine, arginine and proline residues in these enriched proteins. Lysine, arginine and proline were ~11%, 8.5% and 3.7% respectively in both the datasets (Fig. 2C), and (as described earlier), arginine and lysine are substantially over-represented in the ribosomal proteins that form the translation machinery[14]. We separately analyzed a whole-proteome dataset[30], selected the top 500 most abundant proteins and performed a similar analysis

https://doi.org/10.1038/s41467-024-51769-w

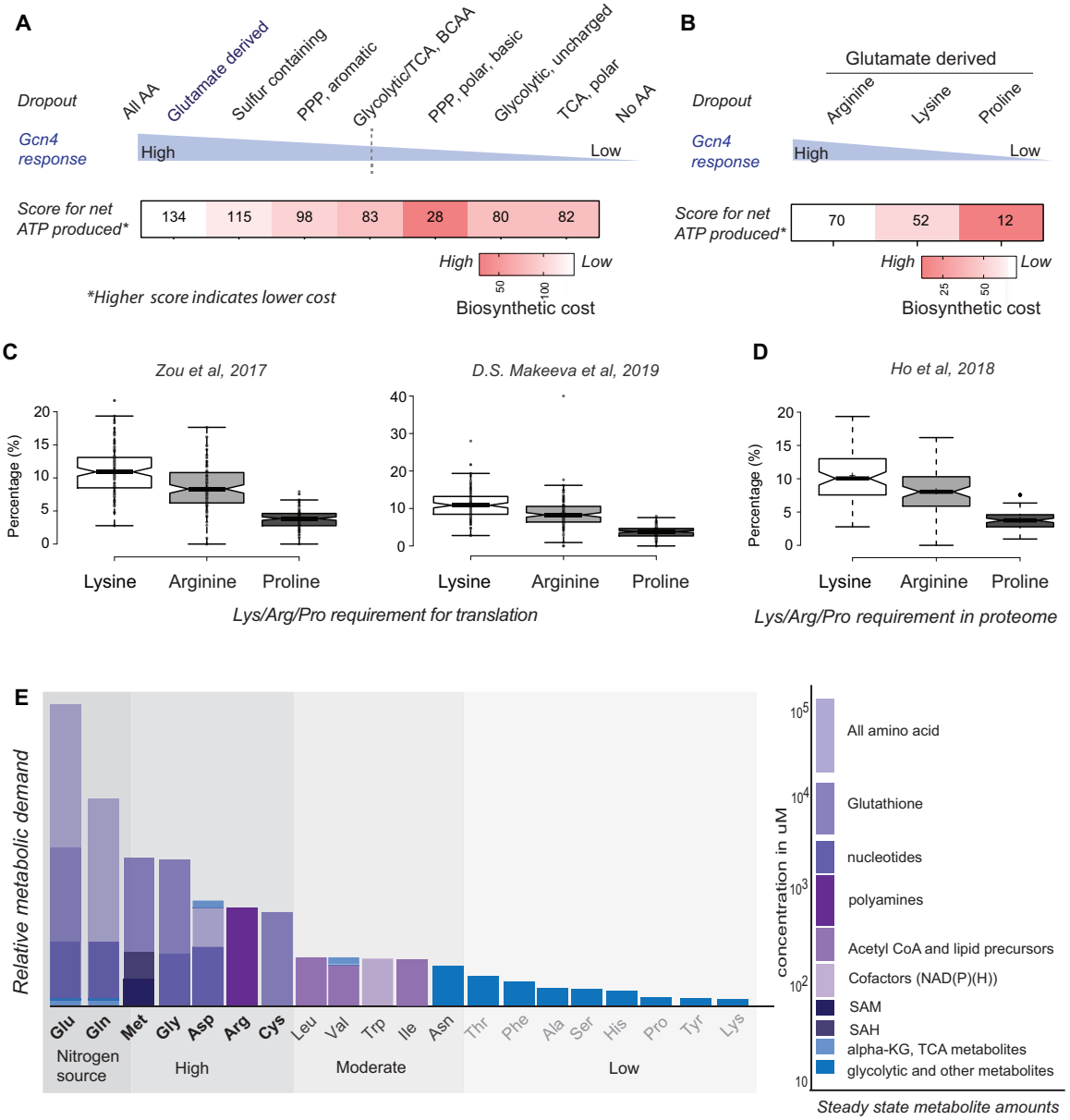

as 2 C. Again, the most enriched GO category was the ribosomal constituents, consisting of >15% of the query genes (Supplementary Fig. S3B). In this abundant protein set, lysine, arginine and proline were ~10.4%, 8.1% and 3.8% respectively (Fig. 2D), consistent with the ribo-seq analysis in Fig. 2C. Together, these results show that the overall (high) demands from protein synthesis for lysine and arginine are comparable, and are ~2–3 times greater than proline requirements.

However, this analysis excludes the metabolic demand component for amino acids. Since there is no current estimate for metabolic demand, we next built a qualitative but composite estimate for the demand for each amino acid, by quantifying the primary metabolic outputs of every amino acid (Fig. 2E, Appendix I, Table S6) (see[31] for a basis of this calculation). Given available data[31], estimates are order of magnitude based. We ranked amino acids from highest to lowest

Fig. 2 | The amino acid restoration response intensity correlates with low biosynthetic cost and high demand. A A consolidated biosynthetic cost analysis for each amino acid group. The consolidated biosynthetic cost of each amino acid group was calculated based on the cumulative number of ATP molecules gained during the biosynthesis of the respective amino acid. The higher score indicates a lower supply cost. See Supplementary Information Appendix 1 for details. **B** Biosynthetic costs for each glutamate-derived amino acid (arginine, lysine and proline), using the cost estimation as in Fig. 2A. The numerical scores indicated within the heat map are as in Fig. 2B. **C** Notched box-plots showing the percentages of lysine, arginine and proline residues in the enriched ribosomal constituents GO category from the highly translated mRNAs ($n = 500$), as assessed from two ribo-seq analyzes datasets. Left panel: data for 134 proteins from Zou et al.[28], where SD footprint reads were analyzed. Right panel: data for 126 proteins from the Makeeva et al.[27], where wt_sd_ribo reads were analyzed. **D** Proteome demand for lysine, arginine and proline. Notched box-plot of the percentages of lysine, arginine, and proline in the enriched ribosomal GO category (75 proteins) from Ho et al.[30]. **E** Quantitative estimates of relative demand for each amino acid in descending order based on their cellular demands, coming from metabolic requirements. The scale bar (in shades of blue) indicates the intracellular concentration ranges of each metabolic output. **F** A summary of the (scaled) demand components for arginine in the cell - coming from protein synthesis requirements, as well as from polyamines synthesis. **G** A proportionally scaled bar summarizing the consolidated demand for each of the glutamate derived amino acids (Arg, Lys, Pro) coming from proteome/translation (greyscale) and metabolic demands (blue and purple, same as (2**E**). The box plots details for (2**C** and 2**D**) are explained in methods. In 2**E**, 2**G**, the size of the bar is in variable units. Data are provided in the Source Data file.

metabolic demand (Fig. 2E), and amino acids fall into clear groups of high, moderate and low demand. This analysis revealed a high metabolic demand for arginine, and low metabolic demands for lysine and proline (Fig. 2E). Arginine is the largest assimilator of nitrogen in cells[32], and much of the demand for arginine comes from its requirement in making polyamines (Figs. 2E, F). Polyamines are abundant cellular metabolites, often present in ~millimolar amounts[33,34]. In contrast, while the demand from protein synthesis for lysine is high, the metabolic demand for lysine is low except in atypical contexts[35]. Finally, the demand for proline in protein synthesis is low, and there is no major metabolic demand for proline under these growth conditions (Figs. 2C–E). Therefore, for the group of glutamate-derived amino acids, the cumulative demand has a major contribution from the high arginine demand, a smaller contribution from the total lysine demand and the smallest contribution from the low demand for proline (Fig. 2G). Summarizing our observations, of the glutamate-derived amino acids, arginine had the lowest biosynthetic costs but the highest demand.

Disrupting arginine supply invokes the strongest response consistent with the law of demand

The magnitude of the restoration response correlated with high demand coupled with low supply costs. In any given nutrient environment, supply parameters are inherent to the physico-chemical properties of that molecule, while demand has added components coming from selection and inherent growth rates for that cell. If these are primary criteria involved, how might cells prioritize an order in which to make amino acids when there are shortfalls? From classical economics, when supply parameters are inherent, the law of demand would drive the economy[36]. According to this law, the demand for an entity and its supply price are inversely correlated, and demand is highest for molecules with low supply costs[36]. In a growing cell, since amino acid amounts are far from equilibrium[1,4], flux would be driven by the law of demand. If so, a hypothetical supply price vs demand curve for the glutamate-derived amino acids could be drawn as in Fig. 3A.

To experimentally test this possibility, we estimated the Gcn4 response to individual dropouts of Arg, Lys or Pro (Fig. 3B). Gcn4 protein was highest in the Arg dropout, as compared to Lys or Pro dropouts (Fig. 3B). Additionally, we estimated transcripts of direct Gcn4 targets. The arginine dropout had the highest response, compared to lysine and proline dropouts (Supplementary Fig. S4A, with controls for Gcn4 mRNA levels shown in Supplementary Fig. S4B). Indeed, this response in the arginine dropout was comparable to complete dropout (-AA) (Fig. 3B). In complementary experiments, we examined 6 h growth in wild-type and *gcn4*Δ cells in individual amino acid dropouts (for Arg, Lys and Pro). *gcn4*Δ cells showed the strongest growth reduction in the arginine dropout (Fig. 3C and Supplementary Fig. S4C). Together, these results indicate that cells are most sensitive to Arg limitation, amongst the glutamate-derived amino acids.

How much of the observed response upon arginine limitation might come from metabolic vs other demands? Is there indeed a large component of arginine demand that comes from metabolism? To estimate this, we established an experiment to address the extent of demand coming from metabolic requirements for polyamines. We used cells which do not have the *ARG1* gene (*arg1*Δ), and which cannot synthesize arginine, and therefore should display a constitutively high Gcn4 response to arginine limitation. Carefully designed add-back experiments, along with the corresponding estimation of Gcn4 protein responses, would allow us to address the contribution of arginine demand from polyamines (Fig. 3D). Using *arg1*Δ cells we first established a time-course to define the arginine addback response in−Arg dropout medium (Supplementary Fig. S4D). The add-back of arginine for ~30 minutes reduced Gcn4 protein to ~basal levels (Supplementary Fig. S4D). Next, we grew *arg1*Δ cells in -Arg medium for 75 min, supplied arginine for 30 and 60 minutes, and harvested cells (using 60 min arginine dropout (-Arg) as a control) (Fig. 3E). Both the 30 and 60 min arginine addback reduced Gcn4 protein levels, with the 60 min add-back resulting in the greatest reduction as compared to the -Arg control (Fig. 3E). With this system established, in order to test the polyamine contribution to the arginine dependent response, we grew *arg1*Δ cells in -Arg medium as earlier (Fig. 3E and Supplementary Fig. S4D) and shifted cells to either arginine supplemented, or to medium supplemented with a major polyamine-spermidine (Fig. 3F). Supplementing spermidine resulted in a ~ 40% reduction in Gcn4 compared to the -Arg control (Fig. 3F, lanes 5 and 6). Expectedly, the arginine addback resulted in a ~complete reduction in the level of Gcn4 (Fig. 3F, lanes 4 and 6). These data suggest that ~half the arginine demand in cells comes from its metabolic requirements. Collectively, these data indicate that restoration-prioritization responses in cells for arginine function in accordance with the law of demand.

Responses of TORC1 activity to supply-disruptions correlate with the law of demand

The activity of the growth-controlling TORC1 pathway reflects the growth-based demand for amino acids, and is highest during rapid cell proliferation (Fig. 4A). If this demand-driven response were universal, whenever the cell needs to readjust demand after a supply disruption, TORC1 activity should reciprocally and proportionally reduce. We therefore assessed the TORC1 response upon transient arginine limitation, using the same experimental set-up as earlier. For this, we examined the phosphorylation status of the classical TORC1 target, Sch9[37], after disrupting the supply of the glutamate-derived amino acids. TORC1 inhibition by rapamycin (which results in dephosphorylated Sch9) was used as a control for lowest TORC1 activity (Fig. 4B). Notably, the largest reduction of TORC1 activity was observed post arginine limitation, as compared to the dropouts of the other glutamate-derived amino acids (Lys or Pro) (Fig. 4B). We also independently assessed another major TORC1 output, which is the induction of ribosomal transcripts[38,39]. Correspondingly, the maximum decrease in ribosomal transcripts (reflecting reduced TORC1 activity) was to arginine dropout (Fig. 4C). Collectively, TORC1 activity shows the greatest reduction upon arginine disruption, and the Gcn4 and

https://doi.org/10.1038/s41467-024-51769-w

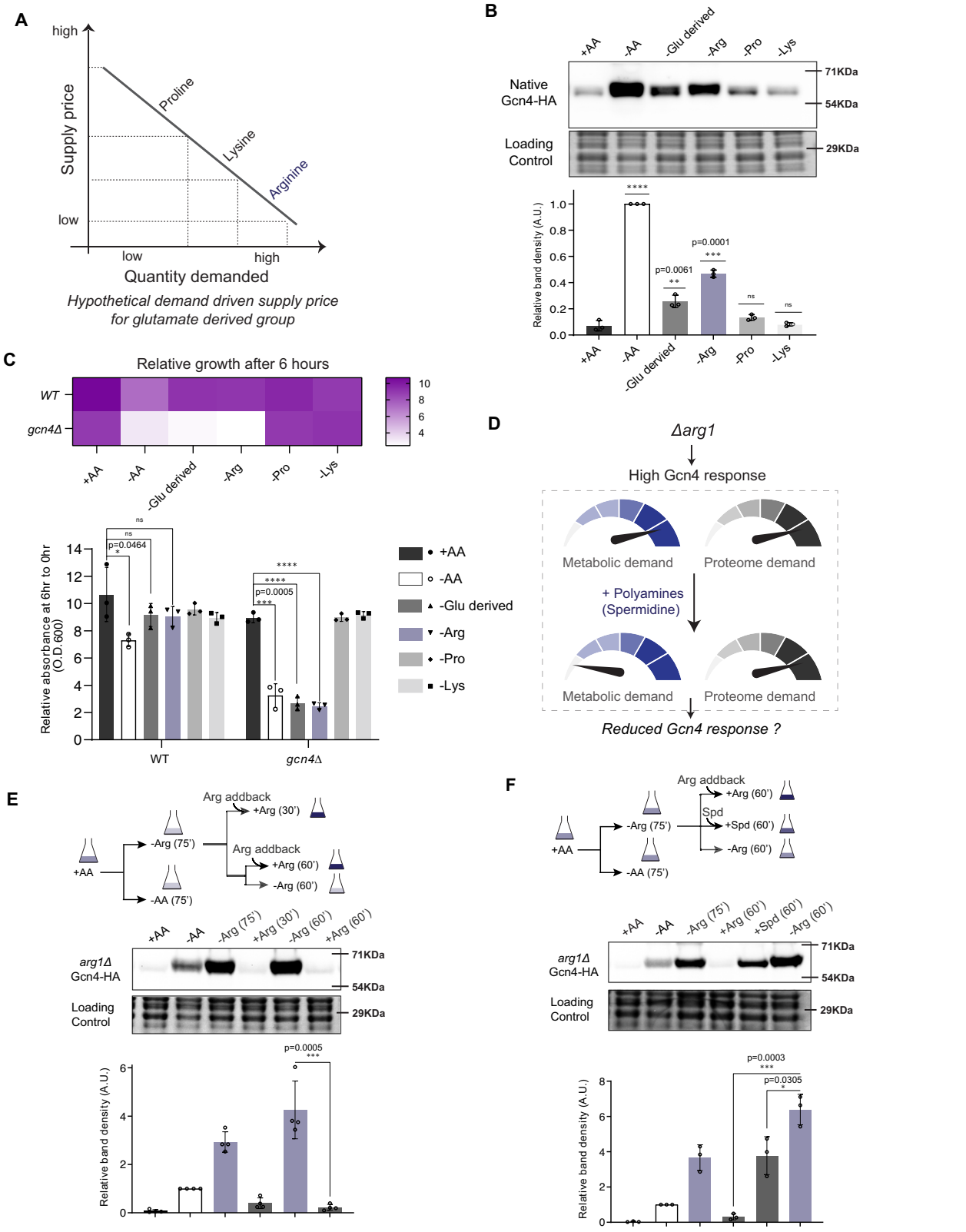

TORC1 responses to arginine are complementary, per the law of demand.

Discussion

In this study, we uncover hierarchical prioritization strategies to restore the supply of *distinct* amino acid groups, when supply is transiently disrupted. If this were organized based on supply costs along with cumulative demand, these data would be consistent with a model illustrated in Fig. 4D. Amino acids with low supply costs, but overall low demand in a given condition will elicit a minimal response because any supply disruption will be quickly restored. In a glucose and nitrogen-replete environment, the glycolysis-derived amino acids have continuous and non-limiting precursor supplies and fit these criteria. Although demand remains high for glutamate/glutamine, in

Fig. 3 | The law of demand drives amino acid restoration-prioritization responses as observed for arginine. A A hypothetical supply price vs required demand graph for the glutamate derived amino acids, as based on the law of demand. **B** Gcn4 response after complete amino acid withdrawal (-AA), or for individual amino acid (Arg, Pro, Lys) dropouts. Relative protein amounts are shown below the representative blot, and comparisons are to +AA. $n = 3$, biological replicates. **C** Relative difference in the growth of wild-type and *gcn4*Δ cells in the indicated amino acid group dropout or complete medium, as estimated after 6 hours. $n = 3$, biological replicates, comparisons are to +AA for WT and *gcn4*Δ sets. **D** A summary of predicted Gcn4 responses in *arg1*Δ (arginine auxotrophic) cells, based on the estimated metabolic and proteome demand for arginine. Since the polyamine contribution towards the arginine demand is high, upon restoring polyamines a reduction in Gcn4 would be predicted. **E** The extent of the Gcn4 response upon arginine deprivation, in arginine auxotrophic cells. The experimental setup is illustrated. The image shows a representative blot for Gcn4 amounts in arginine replete, drop-out, and restored conditions. $n = 4$, biological replicates. **F** The contribution of polyamine synthesis towards the demand for arginine. A representative blot indicating the Gcn4 amounts in minimal medium, or after spermidine (polyamine) supplementation. The experimental set-up is illustrated. $n = 3$, biological replicates. All panels show quantifications displayed as mean ± SEM. Two-tailed student's t-test, $^{****}p < 0.0001$, ns denotes non-significant difference. Data are provided in Source Data file.

the context of this study, the precursor supply is continuous and non-limiting (and they are essentially metabolic sources, as explained in Fig. 1), resulting in a modest response. If per-unit molecule supply costs are high, but demand is low (such as for proline), the limitation of such an amino acid will evoke a minor response regardless of absolute costs to supply each unit, since their supply restorations are easily managed. The strongest responses will therefore be for amino acids with modest individual supply costs, but high demand. This is because while demand is high, supply can still be restored. Such a scenario is exemplified by the response observed for arginine limitation. Based on this framework, there are no amino acids that have high supply costs as well as high demand (Fig. 4D). The prioritization strategies to restore the supply of amino acids therefore correspond to the law of demand, and amino acids form a demand driven economy (Fig. 4D).

It becomes clear that amino acids can be grouped in any way, including the conventional, chemical-structure based grouping, or coarsely by metabolic origin. None of these intuitively indicate supply costs, and for this it is necessary to consider all precursors in a given nutrient environment that go into making the specific amino acid. Additionally, estimating supply costs for individual molecules is relatively straightforward, when the nutrient environment and the active metabolic pathways are mapped out in detail. The costing scale we devise in this study is a useful and easily used example. In contrast, it remains challenging to fully estimate demand costs. In this study, several assumptions were required in order to estimate 'order of magnitude' allocations towards total demand (from a combination of metabolism and protein synthesis). Recent progress now allow excellent assessments of amino acid allocations towards the proteome[6,40,41]. These however miss allocations of amino acids towards metabolism. Contrastingly, systems-level metabolic output predictions do not require quantitative input data for all metabolites[42], and metabolic estimates are derived from 'order of magnitude' calculations[31]. By now including considerations of individual supply-costs and composite demand requirements, we can construct frameworks that suggest prioritization strategies towards distinct amino acids. We hypothesize the following, consistent with the law of demand. First, there are strict chemical constraints imposed in metabolism (based on available substrates, and thermodynamics of reactions), resulting in finite outputs for amino acids[21]. Therefore, this component of amino acid allocations likely has stringent constraints and limited scope for large changes across organisms. Second, the allocations towards the proteome have greater scope for changes, based on the organism and the nature of its environment, growth and other selection. Consequently, across organisms, there can be large variations in proteome allocation strategies, and the cost estimates of supply and demand have to be made accordingly. This implicitly means that the model in Fig. 4D will contextually change primarily in the lower two quadrants (of low costs, and high demand).

Our findings inform two directions of future inquiry. The first predicts what kinds of amino acid reserves might be needed. Intracellular concentrations of different amino acids vary extensively[18], and growing cells maintain excess nitrogen reserves[6]. Including individual supply costs, as well as total demand could help (i) predict prioritization responses as the nutrient environment changes, and (ii) how much amino acid reserves different types of cells might need. An independent line of inquiry asks which amino acids might a cell need to sense? Amino acids are distinct based on metabolic origins, and amounts required. By treating them as distinct entities and not homogenous goods based on these criteria, new and contextual roles for different amino acids can be identified, coming from the demand side, or the supply side. On the demand side, while there are known in vivo TORC1 responses for specific amino acids[43–49], many more responses are observed in vitro, suggesting undiscovered sensing systems. On the supply side, the Gcn2/Gcn4 axis itself can distinguish between individual amino acid groups and is also activated independent of amino acid starvation[50]. We acknowledge that an assessment of such a demand-driven economy can be made more easily for autonomous cells (such as most microbes). However, this becomes very challenging to unravel in complex tissue/organ systems, because of multiple sources of supply, with more complex challenges in estimating elasticity of either demand or supply[3].

Living organisms in Miller's "Living Systems" have been compared to factories, with cells described as open systems, dealing with multiple inputs and outputs of matter, energy and information[51]. In this context, how much can prioritizations of resource restorations be understood based on demand-dependent criteria (or in other words, when would demand dominate)? For cells, a main resource constraint is the input price, which is governed by precursor availability, and rules of chemistry, thermodynamics and evolutionary history. For amino acids, the individual supply prices are fairly constant. Therefore, demand-based criteria would dominate in cells when concentrations of metabolites are saturating (above the enzyme k_m values), and this is typically the case for amino acids, resulting in a demand-elasticity of zero[1–3,52]. In contrasting contexts, where metabolite consumptions are regulated as a function of available supply, supply-based criteria will become increasingly important[3]. Additionally, in a demand-driven context cells must manage the total supply costs because if an input cost is high, the supply is limited since there are boundaries to how much energy can be obtained within cells. An inference from this is that cells would optimize their outputs in tune with these energetic constraints[53,54]. From classical economics, other factors that determine supply prices are: (i) processes used for supply, (ii) anticipation of future prices, (iii) the number of suppliers, and (iv) the presence of monopolies or cartels that restrict supply or increase perceived value of goods[36]. In cells the first (enzymes, transporters) are optimized by selection, evidence for the second is limited to systems exhibiting hysteresis or oscillatory behavior, the third is finite and quantifiable, and the fourth rarely exists. Cells do not consider 'Veblen goods'[55], which have artificially high prices because of perceptions (eg. as status symbols) that manufacture demand. These considerations could therefore help identify resource bottlenecks, as well as likely responses to disruptions in specific resources, and distinguish supply-driven vs demand-driven economies. Work in these areas holds promise to advance a broader understanding of resource allocation strategies in cells, and to improve the metabolic engineering of cell factories.

https://doi.org/10.1038/s41467-024-51769-w

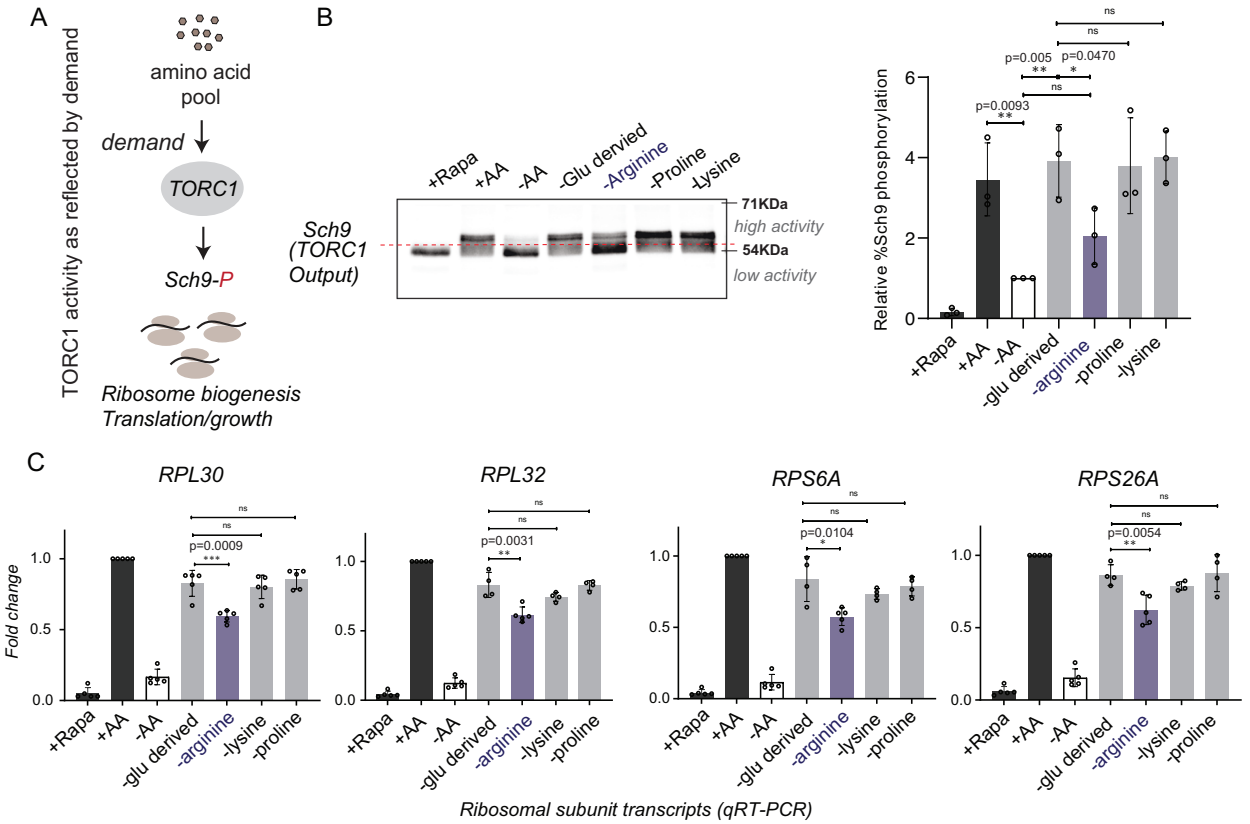

Methods

Yeast strains, media and growth conditions

The prototrophic CEN.PK strain of *Saccharomyces cerevisiae* was used as the wild type in all the experiments. All the strains used in this study are listed in Supplementary Information in Table S1. For cell growth, an overnight preculture was grown at 30 °C (OD_{600} ~ 2) in YPD medium (1% yeast extract, 2% peptone, 2% dextrose), and subsequently sub-cultured in the same medium (starting OD_{600} ~ 0.2) and grown to an OD_{600} ~ 0.55–0.6. Rapamycin treatment: cells were treated with 200 nM rapamycin for 75 min and then harvested. For amino acid limitation experiments, the cells grown as above were washed once with defined minimal medium (0.67% yeast nitrogen base with ammonium sulfate, without amino acids, 2% dextrose) and shifted to this medium supplemented with specified amino acids. Cells were

Fig. 4 | Changes in TORC1 activity upon amino acid supply disruption correlate with the law of demand. A A schematic illustrating the activity outputs of the TORC1. Increased Sch9 phosphorylation and ribosome biogenesis are key readouts of TORC1 activation. TORC1 activity indicates the extent of amino acid demand in a given environment. **B** Assessment of TORC1 activity (based on Sch9 phosphorylation) after transiently disrupting (indicated) amino acid supply. Sch9 phosphorylation was assessed in the indicated amino acid dropouts (Arg, Pro, Lys), based on the electrophoretic mobility of Sch9 in extracts treated with NTCB. A representative blot (from $n = 3$, biological replicates) is shown. Comparisons are to -AA. **C** TORC1 activity as based on ribosomal transcript amounts, after transiently disrupting (indicated) amino acid supply. Relative changes in the expression of the indicated ribosomal subunit transcripts are shown. Comparisons are to +AA, $n \geq 4$, biological replicates. Data for (**4B** and **4C**) are displayed as mean ± SEM, ns denotes non-significant difference, $^{****}p < 0.0001$, Two-tailed student's t-test. Data are provided in the Source Data file. **D** A four-quadrant chart to illustrate the relationship between the cost of biosynthesis/supply for an individual molecule of an amino acid, and the total demand for that amino acid. The size of the circles indicates (relative) intracellular concentrations of the respective amino acid. Based on this framework, amino acids with low supply costs and low demand will elicit a lower restoration response, and amino acids with low supply costs but high demand elicit the highest response. Distinct amino acids populate only three of the four quadrants, to complete the amino acid economy. There are no amino acids which have both high supply costs, as well as high demand in the cell.

grown in this medium for 75 min and then collected. For strains with plasmids, appropriate selection was used during growth. The strains and plasmids used in this study are listed in Supplementary Information Table S1 and S2.

Defined and amino acid dropout medium

For each amino acid dropout medium, all amino acids except the specified dropout were added to a final concentration of 2 mM each except cysteine (final concentration 0.5 mM), and tyrosine was excluded due to its poor solubility. The amino acid dropout media used are listed in Supplementary Information Table S3. For the addback experiments, 10 mM arginine and spermidine were used.

Luciferase reporter assay for Gcn4 activity

The Gcn4 luciferase reporter, and the luciferase reporter assay are as described previously[23,24]. Briefly, wild-type cells transformed with a Gcn4-luciferase reporter (Supplementary Information Table S2) were grown overnight in YPD with G418. Cells were sub-cultured in the same medium without selection and grown till OD_{600} ~ 0.6. 20 ml of this culture was collected ("0 min") and pellets frozen at −80 ^{0}C. The remaining culture was collected, washed and shifted to the specified medium and incubated at 30 ^{0}C for indicated time-points. For the kinetics experiments, cells were harvested after 10, 30, 45, 60, 90, 120, 180 and 240 minutes. Cell pellets were stored at −80 ^{0}C. Pellets were resuspended and lysed in lysis buffer, cleared by centrifugation, and protein concentrations estimated. Luciferase assays were performed using luciferase assay system (E1500, Promega) and activity measured using a Sirius luminometer (Tiertek Berthold). Data was obtained as Relative Light Units per sec (RLU/s). Statistical significance was determined using a Student T-test (GraphPad Prism 10). For single-time point experiments, cells were shifted to the indicated minimal medium, harvested after 75 min and luciferase assays were performed as described.

Addback experiments with arginine and spermidine

Cells were grown overnight and sub-cultured in YPD as described earlier. Cells were washed once with minimal medium and shifted to minimal medium/minimal medium with arginine dropout for 75 mins. At 75 minutes, 20 OD_{600} from the cultures were harvested. The remaining cells were divided for the dropout/addback experiments. For addback experiments 10 mM arginine or spermidine were added at the indicated times, and cells collected for further analysis.

Western blot analysis

Cells were collected, proteins extracted and protein amounts were estimated using Western blotting with specific antibodies, as described earlier[23]. For stabilized Gcn4 protein levels, the SL161 plasmid with stabilized Gcn4-HA (Supplementary Information Table S2) was expressed in *gcn4*Δ strain, and analyzed as described earlier[23]. For steady-state Gcn4 protein levels, Gcn4 tagged at its chromosomally locus with a C-terminal HA epitope was used. See, extended methods (Supplementary Information) for details. Western blots for the Sch9 activity assay are described below.

Sch9 activity assay by NTCB cleavage

For Sch9 detection, Sch9 was tagged at its chromosomal locus with a HA epitope. 10–12 OD_{600} of these cells (grown appropriately) were collected with 6% final concentration of TCA, kept on ice for 15 min, harvested, washed twice with ice cold acetone by centrifugation at 3500 rpm/2000g, 3 min, 4 °C. The cell pellets were dried in a speed-vac for 45–60 min and stored at −80 °C. Cell pellets were resuspended in 300 μl of urea lysis buffer and processed for NTCB (2-Nitro-5-thiocyanatobenzoic acid) cleavage (to assess its phosphorylation status and TORC1 activity) as described previously[37]. Cleaved Sch9 was detected using anti-HA (H6908-.2 ML Sigma-Aldrich) primary antibody and anti-rabbit horseradish peroxidase-conjugated (7074S, Cell Signaling technologies) secondary antibody. See extended methods (supplementary information) for details.

RNA isolation and quantitative real-time PCR (qRT-PCR) analysis

Cells were grown in the specified media, and 5–6 OD_{600} of cells were harvested. RNA was isolated by a hot phenol beating method as described earlier[24], treated with DNAseI (AM2238, Thermo Fisher), cDNA synthesized with random primers (48190011, Thermo Fisher) and SuperScript III reverse transcriptase (18080-085, Thermo Fisher Scientific) according to the manufacturer's protocol. Relative transcript quantifications were done by real-time PCR on an ViiA 7 Real-Time PCR System (Thermo Fisher) using Maxima SYBR Green/ROX qPCR Master Mix (K0222, Thermo Fisher). *ACT1* was used as an internal normalization control. All qRT-PCRs were performed in triplicates using three independent biological RNA samples. Statistical significance was determined using a Student T-test (GraphPad Prism 10).

Relative growth comparisons

WT and *gcn4*Δ cells were grown in YPD and sub-cultured in minimal, dropout or complete medium and cell growth monitored using $O.D_{600}$ for a total of 11 hrs. For final comparisons, relative growth at 0 hr, 6 hr and 11 hr were compared.

Amino acid supply cost calculations

To calculate the biosynthetic cost of each amino acid, we accounted for all the chemical reactions in the biosynthetic pathway of amino acids in cells growing with glucose as the carbon source, ammonium as the nitrogen source. Amino acids are synthesized from the intermediates of the glycolytic pathway, pentose phosphate pathway (PPP), and tricarboxylic acid (TCA) cycle. Based on the nature of the chemical reactions, there is either net 'energy' consumption or production. The energetic cost is in the form of high energy phosphate bonds (ATP), or reducing equivalents (NADH, NADPH). During oxidative phosphorylation, 3 ATP molecules are generated from ~1 NADH molecule. The final consolidated energetic cost for biosynthesis of each amino acid molecule is calculated by estimating the number of net ATP molecules consumed/produced, and by converting the number of the NADH molecules to ATP molecules using the conversion 1 NADH = 3 ATP molecules. In addition to this direct energetic cost, some chemical conversions require other metabolic precursors or cofactors, which

also have associated biosynthetic costs that are included in the calculations. Full details of the amino acid supply cost calculations, as well as the co-factors considered during the synthesis of each amino acid, are available as an extensive document in the Supplementary Information, under Appendix I.

Amino acid demand calculations

Total demand for each amino acid (order of magnitude) was estimated by calculating the allocation of the amino acid for protein synthesis as well as the steady-state proteome, and separately for metabolic uses. Data from two high-quality ribosome-profiling datasets[27,28,30] (GEO accession: GSE91068 and GSE122039) were used for protein synthesis allocations. The top 500 most highly translated genes from these datasets were considered, from which the most enriched gene ontology category was identified, and the percentage composition for each amino acid was estimated. Similarly, from the whole-proteome dataset[30], the top 500 most abundant proteins were selected and analyzed as above for the fractional composition of each amino acid. For the metabolic demand component, we listed (Supplementary information- under Appendix I, Table S6) and then estimated the amounts of the primary metabolic outputs of each amino acid coming from usage estimates from data available[31], and accepted numbers for abundance (https://bionumbers.hms.harvard.edu/search.aspx). We then ranked amino acids from highest to lowest metabolic demand and grouped them into high, moderate and low demand.

Data visualization and statistical analysis

The notched box-plots were constructed using a web-based tool at http://shiny.chemgrid.org/boxplotr/. The upper and lower boxes contain the second and third quartiles and the band gives the median, whiskers extend 1.5 times the interquartile range. If the notches in two plots do not overlap, there is roughly 95% confidence that their medians are different. Gene ontology (GO) analysis was conducted using the web-based tool at https://www.yeastgenome.org/goTermFinder. Quantification of the protein band intensities in Western blots from different biological replicates was done using ImageJ software and statistical significance was determined using Student T-test (GraphPad Prism 10).

Reporting summary

Further information on research design is available in the Nature Portfolio Reporting Summary linked to this article.

Data availability

The authors confirm that the data supporting the findings of this study are available within the study and in the associated Supplementary material. The datasets used in this study are from publicly available datasets (GEO accession: GSE91068 and GSE122039). Source data are provided with this paper.

References

1. Hofmeyr, J. S. & Cornish-Bowden, A. Regulating the cellular economy of supply and demand. *FEBS Lett.* **476**, 47–51 (2000).
2. Hofmeyr, J.-H. S. The harmony of the cell: the regulatory design of cellular processes. *Essays Biochem.* **45**, 57–66 (2008).
3. Ye, J. & Medzhitov, R. Control strategies in systemic metabolism. *Nat. Metab.* **1**, 947–957 (2019).
4. Cornish-Bowden, A. et al. *Biochemical Evolution: The Pursuit of Perfection*. (Garland Science, Taylor & Francis group, 2016).
5. Gutteridge, A. et al. Nutrient control of eukaryote cell growth: a systems biology study in yeast. *BMC Biol.* **8**, 68 (2010).
6. Yu, R. et al. Nitrogen limitation reveals large reserves in metabolic and translational capacities of yeast. *Nat. Commun.* **11**, 1881 (2020).
7. Björkeroth, J. et al. Proteome reallocation from amino acid biosynthesis to ribosomes enables yeast to grow faster in rich media. *Proc. Natl Acad. Sci.* **117**, 21804–21812 (2020).
8. Walvekar, A. S., Srinivasan, R., Gupta, R. & Laxman, S. Methionine coordinates a hierarchically organized anabolic program enabling proliferation. *Mol. Biol. Cell* **29**, 3183–3200 (2018).
9. Boer, V. M., Crutchfield, C. A., Bradley, P. H., Botstein, D. & Rabinowitz, J. D. Growth-limiting intracellular metabolites in yeast growing under diverse nutrient limitations. *Mol. Biol. Cell* **21**, 198–211 (2010).
10. González, A. & Hall, M. N. Nutrient sensing and TOR signaling in yeast and mammals. *EMBO J.* **36**, 397–408 (2017).
11. Valvezan, A. J. & Manning, B. D. Molecular logic of mTORC1 signalling as a metabolic rheostat. *Nat. Metab.* **1**, 321–333 (2019).
12. Hinnebusch, A. G. Evidence for translational regulation of the activator of general amino acid control in yeast. *Proc. Natl Acad. Sci.* **81**, 6442–6446 (1984).
13. Hinnebusch, A. G. Translational regulation of GCN4 and the general amino acid control of yeast. *Annu Rev. Microbiol* **59**, 407–450 (2005).
14. Srinivasan, R., Walvekar, A. S., Rashida, Z., Seshasayee, A. & Laxman, S. Genome-scale reconstruction of Gcn4/ATF4 networks driving a growth program. *PLoS Genet* **16**, e1009252 (2020).
15. Natarajan, K. et al. Transcriptional profiling shows that Gcn4p is a master regulator of gene expression during amino acid starvation in yeast. *Mol. Cell Biol.* **21**, 4347–4368 (2001).
16. Nelson, D. L. & Cox, M. M. *Lehninger Principles of Biochemistry*. (W.H. Freeman, 2017, 2017).
17. Ogata, H. et al. KEGG: kyoto encyclopedia of genes and genomes. *Nucleic Acids Res.* **27**, 29–34 (1999).
18. Bennett, B. D. et al. Absolute metabolite concentrations and implied enzyme active site occupancy in Escherichia coli. *Nat. Chem. Biol.* **5**, 593–599 (2009).
19. Ljungdahl, P. O. & Daignan-Fornier, B. Regulation of amino acid, nucleotide, and phosphate metabolism in *Saccharomyces cerevisiae*. *Genetics* **190**, 885–929 (2012).
20. Wu, G. Amino acids: metabolism, functions, and nutrition. *Amino Acids* **37**, 1–17 (2009).
21. Kirschning, A. On the evolutionary history of the twenty encoded amino acids. *Chem. Eur. J.* **28**, (2022).
22. Rashida, Z. & Laxman, S. The pentose phosphate pathway and organization of metabolic networks enabling growth programs. *Curr. Opin. Syst. Biol.* **28**, 100390 (2021).
23. Walvekar, A. S. et al. Methylated PP2A stabilizes Gcn4 to enable a methionine-induced anabolic program. *J. Biol. Chem.* **295**, 18390–18405 (2020).
24. Gupta, R. et al. A tRNA modification balances carbon and nitrogen metabolism by regulating phosphate homeostasis. *Elife* **8**, e44795 (2019).
25. Mueller, P. P. & Hinnebusch, A. G. Multiple upstream AUG codons mediate translational control of GCN4. *Cell* **45**, 201–207 (1986).
26. Kornitzer, D., Raboy, B., Kulka, R. G. & Fink, G. R. Regulated degradation of the transcription factor Gcn4. *EMBO J.* **13**, 6021–6030 (1994).
27. Makeeva, D. S. et al. Translatome and transcriptome analysis of TMA20 (MCT-1) and TMA64 (eIF2D) knockout yeast strains. *Data Brief.* **23**, 103701 (2019).
28. Zou, K., Ouyang, Q., Li, H. & Zheng, J. A global characterization of the translational and transcriptional programs induced by methionine restriction through ribosome profiling and RNA-seq. *BMC Genomics* **18**, 1–12 (2017).
29. Warner, J. R., Vilardell, J. & Sohn, J. H. Economics of ribosome biosynthesis. *Cold Spring Harb. Symp. Quant. Biol.* **66**, 567–574 (2001).
30. Ho, B., Baryshnikova, A. & Brown, G. W. Unification of protein abundance datasets yields a quantitative saccharomyces cerevisiae proteome. *Cell Syst.* **6**, 192–205.e3 (2018).
31. Milo, R. & Phillips, R. *Cell Biology by the Numbers*. (Garland Science, 2015).

32. Jiranek, V., Langridge, P. & Henschke, P. A. Amino acid and ammonium utilization by saccharomyces cerevisiae wine yeasts from a chemically defined medium. *Am. J. Enol. Vitic.* **46**, 75–83 (1995).
33. Kusano, T., Berberich, T., Tateda, C. & Takahashi, Y. Polyamines: essential factors for growth and survival. *Planta* **228**, 367–381 (2008).
34. Igarashi, K. & Kashiwagi, K. Polyamines: mysterious modulators of cellular functions. *Biochem Biophys. Res. Commun.* **271**, 559–564 (2000).
35. Olin-Sandoval, V. et al. Lysine harvesting is an antioxidant strategy and triggers underground polyamine metabolism. *Nature* **572**, 249–253 (2019).
36. Nicholsan, W. & Snyder, C. *Microeconomic Theory: Basic Principles and Extensions* (11th edn.) (Cengage Learning, 2012).
37. Urban, J. et al. Sch9 is a major target of TORC1 in saccharomyces cerevisiae. *Mol. Cell* **26**, 663–674 (2007).
38. Powers, T. & Walter, P. Regulation of ribosome biogenesis by the rapamycin-sensitive TOR-signaling pathway in saccharomyces cerevisiae. *Mol. Biol. Cell* **10**, 987–1000 (1999).
39. Martin, D. E., Soulard, A. & Hall, M. N. TOR regulates ribosomal protein gene expression via PKA and the forkhead transcription factor FHL1. *Cell* **119**, 969–979 (2004).
40. Metzl-Raz, E. et al. Principles of cellular resource allocation revealed by condition-dependent proteome profiling. *Elife* **6**, e28034 (2017).
41. Kafri, M., Metzl-Raz, E., Jona, G. & Barkai, N. The cost of protein production. *Cell Rep.* **14**, 22–31 (2016).
42. Gu, C., Kim, G. B., Kim, W. J., Kim, H. U. & Lee, S. Y. Current status and applications of genome-scale metabolic models. *Genome Biol.* **20**, 121 (2019).
43. Binda, M. et al. The Vam6 GEF controls TORC1 by activating the EGO complex. *Mol. Cell* **35**, 563–573 (2009).
44. Kingsbury, J. M., Sen, N. D. & Cardenas, M. E. Branched-chain aminotransferases control TORC1 signaling in saccharomyces cerevisiae. *PLoS Genet* **11**, e1005714 (2015).
45. Stracka, D., Jozefczuk, S., Rudroff, F., Sauer, U. & Hall, M. N. Nitrogen source activates TOR (Target of Rapamycin) complex 1 via glutamine and independently of Gtr/Rag proteins. *J. Biol. Chem.* **289**, 25010–25020 (2014).
46. Jewell, J. L. et al. Differential regulation of mTORC1 by leucine and glutamine. *Science (1979)* **347**, 194–198 (2015).
47. Sutter, B. M., Wu, X., Laxman, S. & Tu, B. P. Methionine inhibits autophagy and promotes growth by inducing the SAM-responsive methylation of PP2A. *Cell* **154**, 403–415 (2013).
48. Takahara, T., Amemiya, Y., Sugiyama, R., Maki, M. & Shibata, H. Amino acid-dependent control of mTORC1 signaling: a variety of regulatory modes. *J. Biomed. Sci.* **27**, 87 (2020).
49. Dyachok, J., Earnest, S., Iturraran, E. N., Cobb, M. H. & Ross, E. M. Amino acids regulate mTORC1 by an obligate two-step mechanism. *J. Biol. Chem.* **291**, 22414–22426 (2016).
50. Gupta, R. & Hinnebusch, A. G. Differential requirements for P stalk components in activating yeast protein kinase Gcn2 by stalled ribosomes during stress. *Proc. Natil. Acad. Sci. USA* **120**, e2300521120 (2023).
51. Miller James Grier. *Living Systems*. (Mc-Graw-Hill, University of Minnesota, 1978).
52. van Heerden, J. H., Bruggeman, F. J. & Teusink, B. Multi-tasking of biosynthetic and energetic functions of glycolysis explained by supply and demand logic. *BioEssays* **37**, 34–45 (2015).
53. Cascante, M. The metabolic productivity of the cell factory. *J. Theor. Biol.* **182**, 317–325 (1996).
54. Cascante, M., Marti, E. & Cornish-Bowden, A. *Organization and Regulation of the Metabolic Factory*. in *New Beer in an Old Bottle. Eduard Buchner and the Growth of Biochemical knowledge* 199–214 (Universitat de València, 1997).
55. Phillips, R. J. & Slottje, D. J. The importance of relative prices in analyzing veblen effects. *J. Econ. Issues* **17**, 197–206 (1983).

Acknowledgements

We thank Aswin Seshasayee, Vidyanand Nanjundiah, Orkun Sawyer, Wenying Shou, Vijay Jayaraman and SL lab members for discussions. This research was supported by intramural funding from inStem, a DBT-Wellcome Trust India Alliance Senior fellowship (IA/S/21/2/505922) to SL, and an S. Ramachandran National Bioscience Career Development Award from the Department of Biotechnology, Govt. of India to SL.

Author contributions

S.L. and R.G. conceived the study. R.G., S.A., and S.L. designed experiments. R.G., S.A., and N.D. performed experiments. R.G. and S.A. analyzed data. SL wrote the first draft of the manuscript. S.L., S.A., and R.G. revised the manuscript.

Competing interests

The authors declare no competing interests.

Additional information

Supplementary information The online version contains supplementary material available at https://doi.org/10.1038/s41467-024-51769-w.

Correspondence and requests for materials should be addressed to Sunil Laxman.

Peer review information *Nature Communications* thanks Ruslan Medzhitov, and the other, anonymous, reviewer(s) for their contribution to the peer review of this work. A peer review file is available.